International Journal of Engineering Applied Sciences and Technology, 2018
Vol. 3, Issue 4, ISSN No. 2455-2143, Pages 28-37
Published Online August 2018 in IJEAST (http://www.ijeast.com)

WASTEWATER TREATMENT USING COLUMNS PACKED WITH ACTIVATED CARBON FROM COCONUT WASTE NUCIFERA

Jesús A. Angles Izquierdo
Academic Division of Engineering and Architecture
Juarez Autonomous University of Tabasco
México, Villahermosa, Tabasco

Ebelia del Ángel Meraz
Academic Division of Engineering and Architecture
Juarez Autonomous University of Tabasco
México, Villahermosa, Tabasco

Anabel González Díaz
Academic Division of Engineering and Architecture
Juarez Autonomous University of Tabasco
México, Villahermosa, Tabasco

Faviola González Borraz
Academic Division of Engineering and Architecture
Juarez Autonomous University of Tabasco
México, Villahermosa, Tabasco

Laura Lorena Díaz Flores
Academic Division of Engineering and Architecture
Juarez Autonomous University of Tabasco
México, Villahermosa, Tabasco

***Abstract*—** Activated carbons (CA) were prepared from nucifera Coconuts residues, by chemical activation using H_3PO_4 with concentrations of activating agent the 3.5 M and 5 M, times of impregnation the 24h and 48h and temperatures the 500, 600 and 700°C. The materials obtained were characterized by Fourier Transform Infrared Spectroscopy (FTIR) and Electronic Scanning Microscopy with Dispersive Energy Spectroscopy (SEM-EDS). Packed columns were constructed using the CA with better textural characteristics; the COD adsorption process was evaluated. The CA with better characteristics were classified as mesoporous and presented between 389 and 408 $m^2\ g^{-1}$ surface area, 39-40% yield, COD removal efficiencies (ER) in the range of 75.98-84.1%. The adsorption process with CA was effective for the removal of COD and SST present in the wastewater, under the operating conditions applied.

Keywords—***residual water, Coconut Nucifera, activated carbon, removal, COD***

I. INTRODUCTION

Activated carbon (CA) is a porous material widely used as an adsorbent in different industries [1-2]. It is subjected to activation processes to improve the textural characteristics (greater surface area, volume and pore size distribution) responsible for its adsorbing properties, which allow it to be applied in environmental decontamination processes, catalysis or separation processes, both in the gas phase as in liquid phase [3]. From the industrial point of view CA has many important applications such as: dye removal [4,5,6], metal adsorption [7,8,9], adsorption of ammonia[10,11,12], adsorption of insecticides [13], adsorption of effect [14,15], decrease in odors [16], among others. Its multiple applications have caused that the demand of CA is increasing.

The application of CA in water treatment goes from the elimination of taste and odor to the control of very specific organic compounds. The most common use of CA for wastewater treatment has been in tertiary treatment, after a biological treatment [17] COD is defined as the mass of oxygen consumed by the oxidation of inorganic materials, such as sulfur, nitrite, some metals and organic compounds, and it is often used as a measurement of pollutants in wastewater and natural waters [18]. Several investigations have reported favorable results in the use of CA for the removal of COD [19, 5]

The manufacturing processes of CA can be divided into two types: physical activation and chemical activation [20, 21]. The physical activation takes place in two stages: carbonization and activation of carbonized by the action of oxidizing gases (water vapor, carbon dioxide, air, or mixtures thereof) at high temperatures (400-1000 ° C). In the chemical activation the carbonization and the activation take place in a single stage, the precursor is mixed with an activating agent (phosphoric acid, potassium hydroxide or zinc chloride) and heated in an inert atmosphere, this process is usually carried out at temperatures (400-700 ° C) and lower activation times, producing materials with better textural characteristics compared to physical activation [14, 21]. Prauchner & Rodríguez (2012) [22], found that CA prepared from

International Journal of Engineering Applied Sciences and Technology, 2018
Vol. 3, Issue 4, ISSN No. 2455-2143, Pages 28-37
Published Online August 2018 in IJEAST (http://www.ijeast.com)

physically activated coconut endocarp are materials with relatively low packing densities due to the appearance of empty spaces, while chemical activation with H_3PO_4 reduces the appearance of empty spaces, which consequently are materials with higher packaging density, which positively affects the volumetric adsorption capacity. In addition, the chemical activations lead to lower weight losses during the activation processes and allow the synthesis of carbons with greater mechanical strength and a high proportion of mesopores.

Currently, precursors with a high content of lignin and carbon and low ash contents, such as wood, agricultural residues [1,20], and sewage sludge [16, 23, 24], which guarantee a large-scale sustainable production due to its low cost and high availability [13, 14]. However, there is growing interest in using coconut shells as raw material for CA production, as it is a lignocellulose byproduct [25]. It should be noted that, apart from the nutritious values, shell and coconut shell are very promising sources of CA [13,14]. In this regard, the United Nations Food and Agriculture Organization (FAO, for its acronym in English) reported that in 2013 Mexico was ranked in the ten countries with the highest production of coconut, occupying the eighth position with a production of 1, 170,988 tons [26]. On the other hand, in the processing of the coconut, the pulp and water are used, while the shell constituted by the external cover (exocarp), fiber (mesocarp) and hard shell that encloses the seed (endocarp) has no added value and is considered residual biomass [27]. Therefore, in the present investigation, CA was elaborated from the endocarp of Cocos nucifera chemically activated with H_3PO_4 since this precursor is found in abundance available in Mexico and has very low prices in the local market.

V. MATERIALS AND METHODS

A. Obtaining the raw material

The coconut residues (Cocos nucifera) were provided by small entrepreneurs of Ejido Cuauhtemotzin in the municipality of Cárdenas, Tabasco, México, located at coordinates 18 ° 12'30.42 "North Latitude and 94 ° 6'35.02" West Longitude, characterized by having large surfaces of cocotales. In processing the locals only take advantage of the pulp and coconut water, while the shell constituted by the outer cover (exocarp), fiber (mesocarp) and a hard shell that encloses the seed (endocarp) has no added value and is considered residual biomass [27]. The biomass was transported to the laboratory to make activated carbon, the processing consisted of separating the endocarp, crushing it in grains with sizes between 1.8 and 2 mm in a mill and dry at 105 ° C for 24 hours in an oven [28].

B. Synthesis of activated carbon

The raw material (Cocos nucifera endocarp) was dried and subsequently impregnated with H_3PO_4 as activating agent, with an activating agent/precursor ratio of 2 mL / g, using two concentrations of activating agent (3.5 and 5 M), two times of impregnation 24 and 48 hr. Subsequently, the carbonization was carried out in a muffle at temperatures of 500, 600 and 700 ° C, for one hour. Finally, the obtained coals were washed with abundant water distilled until pH equal to 7 and dried in an oven for 24 hours at 80 ° C. The treatments the resulting results are shown in Table 1.

Table 1. Description of the treatments resulting in the synthesis of CA.

Tratamiento	Descripción
CA1	AA+TI1+C1+TA1
CA2	AA+TI1+C1+TA2
CA3	AA+TI1+C1+TA3
CA4	AA+TI1+C2+TA1
CA5	AA+TI1+C2+TA2
CA6	AA+TI1+C2+TA3
CA7	AA+TI2+C1+TA1
CA8	AA+TI2+C1+TA2
CA9	AA+TI2+C1+TA3
CA10	AA+TI2+C2+TA1
CA11	AA+TI2+C2+TA2
CA12	AA+TI2+C2+TA3

C. Surface area analysis

The analysis was carried out in a Micromeritics TriStar II gas adsorption device. For the analysis, 200 mg of CA were weighed, each sample was degassed at 573 K (300°C) with N_2 flow for 2 hours, then adsorption-nitrogen desorption isotherms were taken at 77 K (-196°C) and based on the results obtained, the specific surface area was calculated applying the BET model.

D. Fourier transform infrared spectroscopy (FTIR)

The CA samples were structurally characterized by Fourier transform infrared spectroscopy (FTIR). The samples were mixed with KBr (Sigma Aldrich grade FTIR) at a concentration of 5% w/w and pressed to obtain pellets. Subsequently, they were analyzed in a Shimadzu Model Affinity FT-IR spectrometer (Shimadzu Scientific Instruments, Columbia, MD, U.S.A.), in a range of 340-4700 cm^{-1}, at a resolution of 2 cm^{-1} and 40 scans. The data was processed in the IrsolutionSoftware ™

V. Scanning electron microscopy (SEM)

The CA samples were analyzed by scanning electron microscopy (SEM). For morphological analysis, the samples were mounted on double-sided copper conductive tape in an aluminum sample holder. Subsequently, JEOL JSM-6010LA (JEOL Technics Ltd., Tokyo, Japan) was observed in a scanning electron microscope at 20 kV acceleration voltage under high vacuum conditions at 150X and 5000X. A

International Journal of Engineering Applied Sciences and Technology, 2018
Vol. 3, Issue 4, ISSN No. 2455-2143, Pages 28-37
Published Online August 2018 in IJEAST (http://www.ijeast.com)

dispersive energy detector (EDS) coupled to the SEM was used to perform the semiquantitative analysis and distribution of elements on the surface of the samples. The images were processed in the InTouchScope™.

V. Residual water characterization

The residual water was sampled in the influent of a wastewater treatment plant (WWTP) of a higher education institution, the sampling frequency was carried out following the specifications of NOM-001-SEMARNAT-1996 [29] (SEMARNAT, 1996). The discharge generating process operates for approximately 10 hours, so a sampling interval of 2.5 hr was used, obtaining 4 simple samples that were subsequently mixed to obtain a composite sample, for the =sampling the analytical routines of the [30] NMX-AA-003. The residual water sample was characterized physicochemically, the temperature was determined [31] (NMX-AA-007, a visual method with a thermometer), pH [32] (NMX-AA-008, potentiometric method), COD [33] (NMX-AA-030, spectrophotometric method) and total suspended solids (NMX-AA-034, gravimetric method).

G. Evaluation of the adsorption process

To evaluate the adsorption process, two columns were constructed that operated in parallel and with upward flow using a diaphragm pump following the methodology of [19]. An expense of 3 ml /min was used with the contact time of 8 hours. In each column, the COD was determined, in the influent and in the effluent, every 7 hours for 100 hours to know the removal capacity of this basic contaminant and to identify the saturation time of the CA. At the end of the test, temperature, pH and total suspended solids were determined in the effluent of the columns, were washed with abundant distilled water until pH 7 and dried in an oven for 24 hours at 80 ° C. The resulting treatments are shown in Table 1.

II. EXPERIMENT AND RESULT

A. Caracterización textural

In Figure 1, the N_2 adsorption isotherms at 77 K are shown for CA prepared from coconut shell. According to the classification of isotherms according to the form, all the isotherms obtained were typed I, which are given by microporous solids that have relatively small external surfaces this is a characteristic of activated carbons, zeolites and certain porous oxides [34]. The textural properties of the Cas are related to their adsorbent capacity, Njoku *et al.* (2014) [13] mention that the accessibility of organic molecules to pores depends on their size.

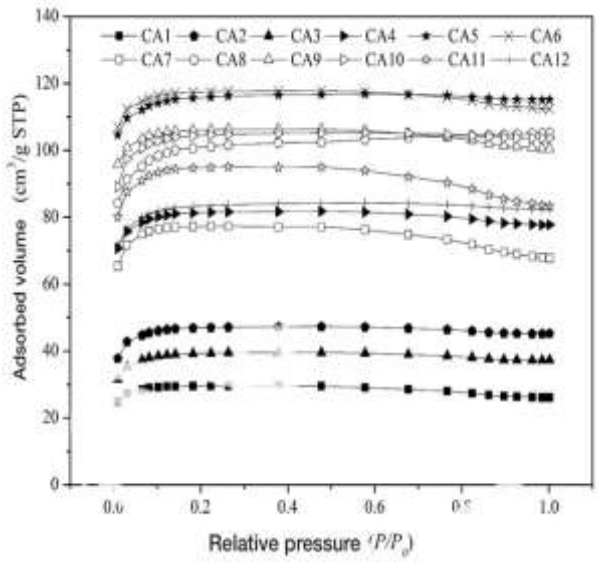

Figure 1. Adsorption isotherms with N_2 at 77 K of the CA.

The Cas that had the largest surface area were CA5 and CA6, so they were selected to be evaluated in the adsorption process in packed columns for wastewater treatment (Table 2).

Table 2. Surface area and yield of CA obtained from the endocarp of Cocos nucifera and H_3PO_4.

CA	Superficial area (m^2 g-1)	Performance (%)
CA1	98.9742	34.687
CA2	158.4741	37.736
CA3	133.1346	39.069
CA4	273.7315	38.395
CA5	389.7644	40.617
CA6	408.706	39.717
CA7	259.0823	41.900
CA8	343.5531	40.317
CA9	355.2813	39.848
CA10	352.1789	49.829
CA11	320.3624	47.976
CA12	281.6673	42.584

It is important to note that the surface area was considered as a substantial parameter for the adsorption process in columns, since according to Rout *et al.*, (2015) [35], it is a main physical property to regulate the adsorption of chemical compounds. It should be noted that the surface area values obtained are greater than those reported by Ouyang *et al.* (2013) [36], with 10-229 m^2/g in CA prepared with coconut husk and pyrolyzed at temperatures in the range of 300-700 ° C, are also higher than those obtained by Shamsuddin *et al.* (2016) [21] with 13.68 and 299.02 m^2/g in CA prepared with H_3PO_4, and similar to those reported by Ensuncho *et al.*

International Journal of Engineering Applied Sciences and Technology, 2018
Vol. 3, Issue 4, ISSN No. 2455-2143, Pages 28-37
Published Online August 2018 in IJEAST (http://www.ijeast.com)

(2015) with 334 m^2/g in CA elaborated from coconut husk, by Njoku *et al*. (2014) [13] with 483.64 m^2/g in CA made with precursors of coconut and H_3PO_4 and by Rout *et al*., 2015[35] with averages of 515 m^2/g in CA made with coconut shell and pyrolysed at temperatures in the range of 450-600 ° C, whereas Bastidas *et al.* (2010) [28] reported 701.98 m^2/g in CA prepared from coconut husk and H_3PO_4, these results can be associated with activation and concentration conditions of the activating agent that have a great influence on the surface area [38]. It is possible that this effect is associated with the process of dehydration by the activating agent, which increases the surface area and porosity, in addition to the H_3PO_4 inhibiting the formation of tars and any other liquid that could clog the pores of the sample, favoring that the volatile movement through the porous is not hindered [39, 40 41]. On the other hand, Ouyang *et al*. (2013) [36] mention that the increase in surface area, total pore volume, and micropore volume is related to the increase of the pyrolysis temperature during the process, since it is the result of the evolution of the volatile components on the material, in addition, they point out that the porosity, especially the microporosity developed around 600 °C, is related to the evolution of hydrogen gas. The percentage of yield in the CA, obtained by relating the weight of the precursor material (Cocos nucifera endocarp) and the weight of the porous solid obtained at the end of the process, varied between 34.68% and 49.82% (Table 2). Shamsuddin *et al*. (2016) [21], affirm that high content of volatile material reduces the yield of solids in the carbonization stage, while a low inorganic content is essential due to its ability to produce low ash content and high carbon content.

B. Infrared spectroscopy with Fourier transform (FTIR)

The functional groups present on the surface of the Cas play an important role in the adsorption of organic and inorganic contaminants [8]. Figure 2 shows the FTIR spectra of the precursor (Cocos nucifera endocarp) and the Cas.

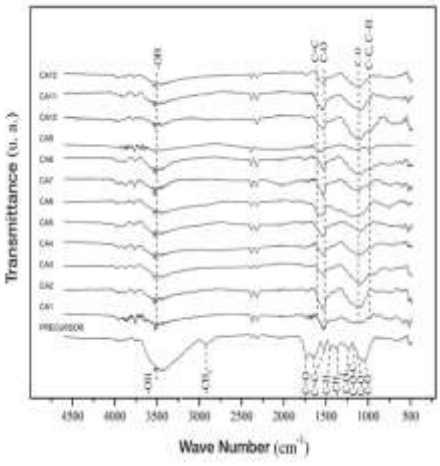

Figure 2. FTIR spectra of the precursor and the CA.

In the precursor a wide band is distinguished to 3423.8 cm^{-1} attributed to hydroxyl groups (stretch –OH) that are due to the presence of moisture and carboxylic acids present in proteins and carbohydrates [42], the bands 2923.25 and 1245.36 cm^{-1} are due to the vibration of tension and flexion in the plane of the groups $–CH_2-$ and CO, respectively, in esters (= COC); These groups are characteristic in cellulose. The bending in the plane at 1446.67 cm^{-1} and the symmetrical bending at 1373.38 cm^{-1} indicate the presence of groups C-H and CH_3, respectively.The bands at 1639.56 and 1517.08 cm $-^{1}$ are attributed to the tension vibrations own of C=C. The band at 1738.90 cm^{-1} is attributed to the presence of C=O in aldehydes and lactones. The signal at 1057.04 cm^{-1} corresponds to CO in phenols (C-OH, primary), the signal to 1117.40 cm^{-1} is due to CO in phenols (secondary C-OH), and 1155.13 cm $^{-1}$ corresponds to C-O-C, it should be noted that the functional groups identified in the precursor are susceptible to react with acids and bases [8]. After activation with H_3PO_4, you can see that many characteristic bands disappear while keeping the signal of stretch vibration of the hydroxyl groups (-OH to 3421 cm^{-1}) but with lower intensity since they are denaturing and breaking the characteristic links and disintegrating the species that do not support the pyrolysis temperature [21, 35, 36, 39, 42], the band that corresponds to the stretching of C = C of aromatic rings (1600 cm^{-1}) and C-O in primary R-OH (1080 cm $^{-1}$). The signals around 2350 cm^{-1} , are characteristics of the tension vibrations asymmetric of the CO_2 molecule. The band at 1510 cm^{-1} is attributed to carboxyl structures carbonate. The signal around 1150 cm^{-1} corresponds to the vibration of C-O stretching in alcohols, phenols, ethers or esters and the band at 970 cm^{-1} is associated with the vibration of stretching of C-C or C-H groups [9]. The signal in the precursor around 1730 cm^{-1} of the C=O group of substituted carboxylic acids, was absent in the CA, this because as the calcination temperature increases the carboxyls present are they gradually dissociate [42], he stressed that the spectra of the different CA presented the same bands but with different intensity, in this respect Shamsuddin *et al*., (2016) [21] mention that the intensity of the band is a function of the activation temperature.These results show that activation with H_3PO_4 promotes chemical changes in the structure of the precursor during pyrolytic decomposition, promoting dehydration and redistribution of the constituents of the Cocos nucifera endocarp (lignin, cellulose and hemicellulose), favoring the conversion of the aliphatic compounds to aromatics obtaining mainly polyaromatic Cas [8].

C. Morphological analysis by scanning electron microscopy

Figure 3 shows the micrographs that reveal the morphology of the precursor and the CA prepared, in which you can compare the external structures of these materials and exposes the alteration of the physical structure of the precursor. The

International Journal of Engineering Applied Sciences and Technology, 2018
Vol. 3, Issue 4, ISSN No. 2455-2143, Pages 28-37
Published Online August 2018 in IJEAST (http://www.ijeast.com)

external structure of the precursor (Figures 3a and 3b), has an aspect of folds in irregular shape with some grooves and few pores are accounted for in the particles, the higher approach is observed a compact structure, which indicates that from the point of view morphological, it is a material with little porosity. On the other hand, the external structure of the Cas prepared (Figure 3c and 3e) presents a widely developed macroporous network, with a presence of channels that according to Zhu & Kolar (2016) [25], can have an interrelated texture with mesopores, which help transport adsorbent to the interior of the carbon particle and they facilitate the adsorption of pollutants. Likewise, the closer (Figure 3d and 3f) observe a large number of macropores, which demonstrates the effect of the activating agent (H_3PO_4) and the pyrolysis treatment that due to dehydration increase the porosity in the structure of the precursor [13, 36, 40, 41, 43, 44, 52] found that the Cavities formation can be related to the expulsion of gases or vapors and Volatile compounds during the calcination processes.

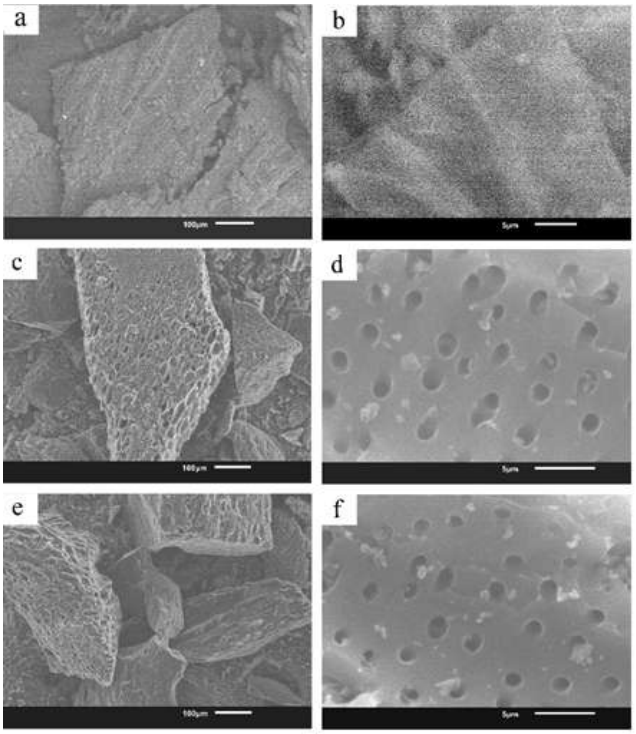

Figure 3. Micrographs (SEM) of the external structure of the precursor (a and b) and of the activated carbons CA5 (c and d) and CA6 (e and f).

Indeed, the presence of smaller particles observed in Figures 3d and 3f can be attributed to the volatile compounds during the carbonization process [25]. In general, in all the particles of the CA, pores of different magnitudes were observed, which could contribute to the increase of the surface area of the materials and fulfill important functions in the processes of adsorption of molecules [21, 25, 35, 37].

D. Elementary microanalysis by EDS

The microelements analysis by EDS was carried out in order to establish a profile of global composition of CA samples. Figure 4 shows the spectrum obtained with their respective emission lines; qualitatively, it is emphasized that CA samples do not have detectable impurities, since only two lines were fully identified corresponding to characteristic carbon emissions I (transition Kα to 0.277 keV) and oxygen (O) (transition Kα to 0.525 keV), which indicates an adequate cleaning of the samples.

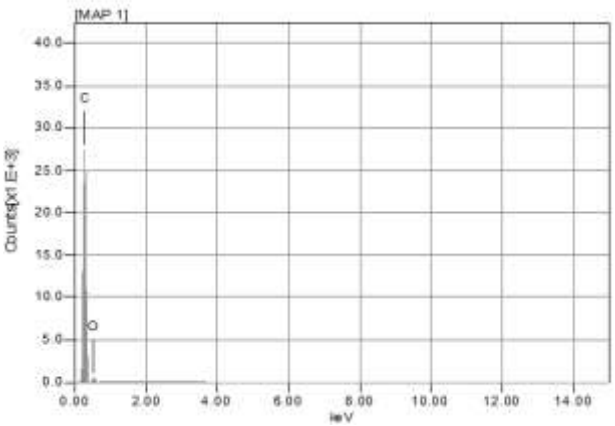

Figure 4. The spectrum of the SEM-EDS type microanalysis of the CA samples.

While in the precursor, the presence of C, O, P and K was identified, the latter they represented 1.31% more of the total composition. Initially, the composition of the precursor comprised about 55% more C and 43% more O, after calcination, the concentration of C increased and that of O decreased. Primera *et al*. (2011) [39], mention that the increase in carbon content is due to the dehydrating nature of phosphoric acid, which facilitates the loss of hydrogen and oxygen, and converts large carbon units into units smaller with greater carbon richness. The content of C in the CA oscillated between 81.42-92.34% ms and that of O between 7.66-18.58% ms (Figure 5), the highest contents of C corresponded to CA prepared at higher activation temperature, similar results were reported by Sulistyani *et al*. (2015) [45] who obtained higher contents of C a higher activation temperature in CA made from coconut shell. I also know observed that the percentage of C was higher in CA prepared with higher ratio of H_3PO_4, to respect Li *et al*. (2011) [46] reported higher contents of C in the pores of CA compared to the surface of the same, effect that attributed to a chemical modification due to the reaction between the carbon and the acid, which took place mainly in the pores of the CA.

International Journal of Engineering Applied Sciences and Technology, 2018
Vol. 3, Issue 4, ISSN No. 2455-2143, Pages 28-37
Published Online August 2018 in IJEAST (http://www.ijeast.com)

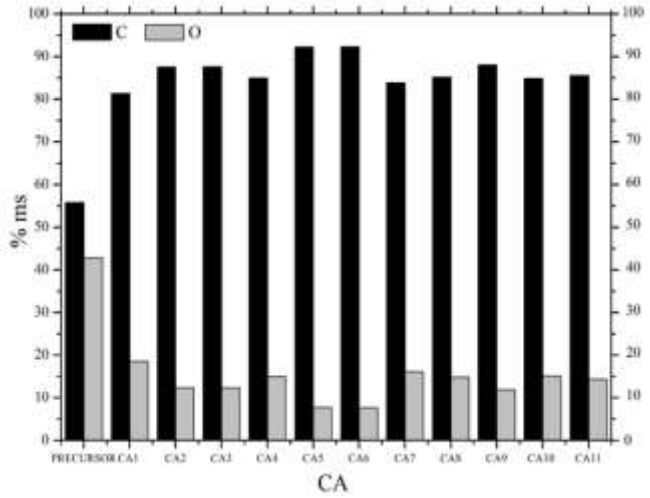

Figure 5. Quantitative elemental microanalysis (% ms) performed by SEM-EDS in precursor and CA samples.

In this sense, the high contents of C in CA5, CA6, and CA12 can be associated to materials with high macroporous structure, which is in accordance with the morphological analysis made to these materials (Figure 5). The dispersion of C was observed by mapping the chemical composition in the SEM, in this, it is possible to determine the dispersion of each element present in the sample. Figure 6 shows the mapping images for the CA5 and CA6 samples. It can be seen that both carbonaceous materials show a homogeneous dispersion of C, without formation of agglomerates or shortages thereof.

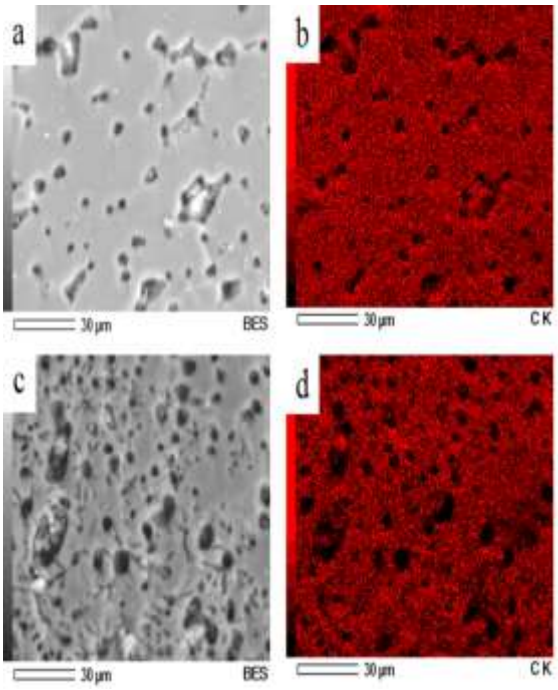

Figure 6. SEM-EDS elemental composition maps of activated carbons CA5 (a and b) and CA6 (c and d).

E. Evaluation of the adsorption process

After one hundred hours of use, the removal efficiencies (ER) of SST and COD were evaluated. Table 3 shows the chemical parameters of the wastewater in the influent and effluent of the columns packed with CA5 and CA6 and the Ers for 8 hours of retention time. The pH values in the effluent of the columns were maintained between 6 and 7 units, so this parameter meets the permissible range imposed in the official Mexican regulations for discharges. In all the columns positive efficiencies were obtained in the removal of SST, indicative of the good performance of carbonaceous materials; however, this parameter was greater in the columns packed with CA6. At the end of the evaluation, CA5 managed to remove 19.11 and 24.84 mg/L of TSS, while CA6 removed 64.00 and 67.82 mg / L of TSS. At the end of the trial, the COD Ers were also positive, which indicates that the material has not yet reached its saturation, which suggests evaluating the materials for more time of use. In this regard, Vacca *et al.*, (2012) [47] mention that a negative removal efficiency is associated with the desorption process, which is carried out once the adsorbent column is saturated, increasing the concentration in the effluent.

Table 3. Chemical parameters of the wastewater in the influent and effluent of the columns packed with CA5 and CA6 and removal efficiencies after one hundred hours of use.

Parameter (Unity)	Wastewater (influent columns)	CA5		CA6	
		Effluent Column 1	Effluent Column 2	Effluent Column 1	Effluent Column 2
Temperature (°C)	29	25	25	25	25
pH	7.92	6.93	6.37	6.59	6.63
COD(mg/L)	670.48	465.07	500.11	458.55	479.22
TSS (mg/L)	179.56	160.45	154.72	111.74	115.56
ER* TSS (%)	----	10.64	13.83	37.77	35.64
ER COD (%)	----	30.63	25.41	31.60	28.52

The adsorption capacity of this material is not only based on its structure but on the versatility that has to be modified by impregnation of chemical agents. The results obtained in Table 2 indicated a higher percentage of yield in the samples CA10 and CA11 that go of 49.829% and 47.976% respectively, the CA2 reported 37.736%. Rodríguez *et al*., (1998) [48] relates the performance with the concentration of pregnant and pyrolysis temperature, due to the dehydrating nature of the phosphoric acid that facilitates the loss of hydrogen and oxygen increasing the carbon in the samples, the hydrolysis of the lignin increases the performance and porosity of the material. Ouyang *et al*., (2013) and Huidobro *et al*., (2000) [36,49] indicate that the loss of water in the pyrolysis process allows the decomposition of polyphosphoric acids from temperatures higher than 600°C. The CA5 and

International Journal of Engineering Applied Sciences and Technology, 2018
Vol. 3, Issue 4, ISSN No. 2455-2143, Pages 28-37
Published Online August 2018 in IJEAST (http://www.ijeast.com)

CA6 showed greater surface area, this increase was related to the temperature of pyrolysis, which was 600-700°C.

Figure 2 of graphical FTIR spectra shows acidic and basic functional groups characteristic in activated carbons, such as the carbonyl group (C=O), carboxyl (CO), hydroxyl (OH -), lactin, quinine [11] and among the basic groups we can mention pyrone and chromene [50]. Which help the material selectively adsorbs certain compounds. Table 3 shows the results obtained in each of the columns of CA5 and CA6 after 100 hours of operation, where the exit concentration depended on the adsorption capacity of each column. The specific surface of the material can be represented as the molecular sheets that are held together by chemical bonds. When the impurities are adsorbed they get trapped on the surface of this structure forming physical unions with coal [51]. Carbon atoms exist in the internal surface of the coal exert an attraction (van der Waals forces) on molecules of the surrounding liquids and gases. The CA5 managed to remove 170.3 and 205.41 mg/L of COD, while CA 6 removed 191.26 and 211.93 mg/L of COD (Figures 7 and 8).

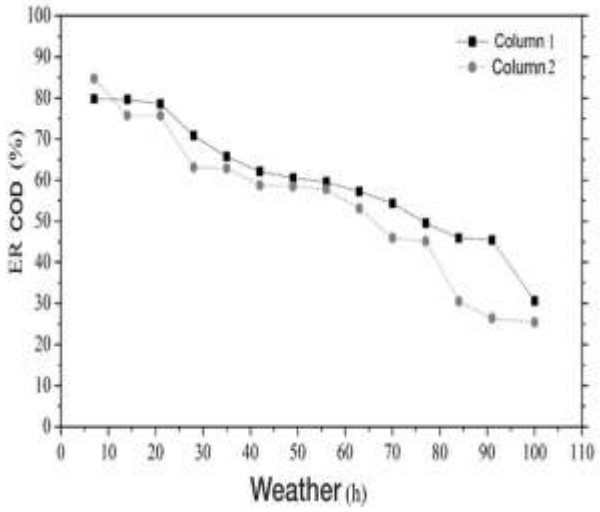

Figure 7. DQO removal efficiency curve in columns packed with CA5.

In the first seven hours of evaluation the columns had ER average of COD of 75.98% to 84.91%, respectively, half of the evaluation, as expected, the ER COD decreased; however, at this time the columns packed with CA6 showed higher ER of COD compared to those packed with CA5, this effect can be reflected in the lower slope of the CA6 efficiencies curves in the first 50 h (Figure 8).

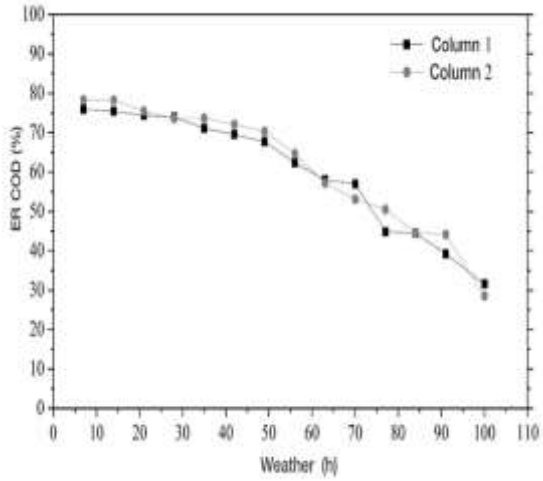

Figure 8. DQO removal efficiency curve in columns packed with CA6

If it is taken into account that the COD in the influent of the columns was 670.48 mg /L, the effluents from the columns are still very polluting (although the COD is not regulated),what is needed of other complementary treatment before or after, in order to have the water treated by this route. In this regard, Méndez *et al.* (2002) [19] mention that a reduction of pH it helps considerably to increase ER of COD in carbonaceous materials, an effect that they associate with that a lower pH causes the colloidal particles to destabilize and form microflocles which are removed by coal

IV.CONCLUSION

Mesoporous Cas were obtained, with highly developed macropore structure and good textural properties, which give it adsorption capacity. The use of columns of adsorption packed with granular CA prepared from Cocos nucifera endocarp and H_3PO_4, achieved the removal of 10-35% SST and COD 25-31.60% of wastewater without previous treatment, the evaluation of the adsorption process showed that the evaluated materials. They have an adsorption capacity even after one hundred hours of use. The ability was demonstrated adsorbent of the synthesized CA, which can be applied for the treatment of water in PTAR, including a previous or subsequent treatment to improve the quality of the water treated by this route, in addition to considering the operational parameters as operating expense and time of saturation, which may limit its effectiveness.

V. REFERENCE

[1] Saka C. "BET, TG–DTG, FT-IR, SEM, iodine number analysis and preparation of activated carbon from acorn shell by chemical activation with $ZnCl_2$". *Journal of Analytical and Applied Pyrolysis*, Vol. 95, 21 24, 2012.

[2] Gokce Y. & Aktas Z. "Nitric Acid Modification of Activated Carbon Produced by Waste Tea and Adsorption of Methylene Blue and Phenol". *Applied Surface Science,* Vol. 313, 352-359, 2014.

[3] Zhu Y. & Kolar P. "Investigation of adsorption of p-cresol on coconut shell-derived activated carbon". *Journal of the Taiwan Institute of Chemical Engineers*, Vol. 68, 138-146, 2016.

[4] Goswami M. & Phukan P. (2017). Enhanced adsorption of cationic dyes using sulfonic acid modified activated Carbon. Journal of Environmental Chemical Engineering, 5, 3508-3517.

[5] Ghani ZA., Yusoff M.S., Zaman N.Q., Zamri M.F. & Andas J. (2017). Optimization of preparation conditions for activated carbon from banana pseudo-stem using response surface methodology on the removal of color and COD from landfill leachate. *Waste Management*, 62,177-187.

[6] Islam M.A., Ahmed M.J., Khanday W.A., Asif M. & Hameed B.H. (2017). Mesoporous activated coconut shell-derived hydrochar prepared via hydrothermal carbonization-NaOH activation for methylene blue adsorption. *Journal of Environmental Management*, 203, 237-244.

[7] Amuda O.S., Giwa A.A. & Bello I.A. (2007). Removal of heavy metal from industrial wastewater using modified activated coconut shell carbon. Biochemical Engineering Journal, 36:174-181.

[8] Lavado-Meza C., Sun-Kou M.R. & Bendezu S. 2010. Adsorción de plomo de efluentes usando carbones activados con H_3PO_4. Revista de la Sociedad Química del Perú, 76 (2) ,165-178.

[9] Sumrit M., Phansiri M., Wanwimon P. & Sataporn K. (2015). Characterization and Properties of Activated Carbon Prepared from Tamarind Seeds by KOH Activation for Fe (III) Adsorption from Aqueous Solution. The Scientific World Journal Article ID 415961.

[10] Guo J., Xu W.S., Chen Y.L. & Lua A.C. (2005). Adsorption of NH3 onto activated carbon prepared from palm shells impregnated with H2SO4. Journal of Colloid and Interface Science, 28, 285-290.

[11] Huang C.C., Li H.S. & Chen C.H. (2008). Effect of surface acidic oxides of activated carbon on adsorption of ammonia. Journal of Hazardous Materials, 159, 523-527.

[12] Yonghou Xiao, Shudong Wanga, Diyong Wua, Quan Yuana. (2008). Experimental and simulation study of hydrogen sulfide adsorption on impregnated activated carbon under anaerobic conditions Journal of Hazardous Materials Volume 153, Issue 3, 30 May 2008, Pages 1193-1200,

[13] Njoku V.O., Azharul-Islam M., Asif M. & Hameed B.H. (2014). Preparation of mesoporous activated carbon from coconut frond for the adsorption of carbofuran insecticide. Journal of Analytical and Applied Pyrolysis, 110, 172-180.

[14] Hidayu A.R. & Muda N. (2016). Preparation and characterization of impregnated activated carbon from palm kernel shell and coconut shell for CO_2 capture. Procedia Engineering, 148, 106-113.

[15] Sawant S.Y, Munusamy K., Somani R.S., John M., Newalkar B.L. & Bajaj H.C. (2017). Precursor suitability and pilot scale production of super activated carbon for greenhouse gas adsorption and fuel gas storage. Chemical Engineering Journal, 315, 415-425.

[16] Lebrero R., Rodríguez E., García-Encina P.A. & Muñoz R. (2011). A comparative assessment of biofiltration and activated sludge diffusion for odour abatement. Journal of Hazardous Materials, 190, 622-630.

[17] Crites R. & Tchobanoglous G. (2000). Sistemas de manejo de aguas arbon ls para núcleos pequeños y descentralizados. Tomos 1, 2 y 3, Bogotá Colombia, Mc Graw Hill.

[18] American Public Health Association (APHA). (1998). Standard Methods for the examination of arbo and wastewater. (20th Ed.), American public health Association, American Wáter Works Association, and Wáter Environmental Federation. Washington.

[19] Méndez-Novelo R.I., Medina-Hernández E., Quintal-Franco C., Castillo-Borges E.R. & Sauri-Riancho M.R. (2002). Tratamiento de lixiviados con carbon activado. *Ingeniería*, 6(3), 19-27.

[20] Yahya M.A., Al-Qodah Z., Ngah C.W.Z. (2015). Agricultural bio-waste materials as potential sustainable precursors used for activated carbon production: A review. Renewable and Sustainable Energy Reviews, 46, 218-235.

[21] Shamsuddin M.S, Yusoff N.R.N. & Sulaiman M.A. 2016. Synthesis and characterization of activated carbon produced from kenaf core fiber using H3PO4 activation. Procedia Chemistry, 19, 558-565.

[22] Prauchner

[23] Al-Qodah1 Z. & Shawabkah R. (2009). Production and characterization of granular activated carbon from activated sludge. Brazilian Journal of Chemical Engineering, 26(01):127-136.

[24] De Filippis P., Di Palma L., Petrucci E., Scarsella M. & Verdone N. (2013). Production and Characterization of

Adsorbent Materials from Sewage Sludge by Pyrolysis. C*hemical Engineering Transactions*, 32,205-210.

[25] Zhu Y. & Kolar P. (2016). Investigation of adsorption of p-cresol on coconut shell-derived activated carbon. Journal of the Taiwan Institute of Chemical Engineers, 68, 138-146.

[26] FAO (2013). Organización de las Naciones Unidas para la Alimentación y la Agricultura (FAOSTAT). Clasificaciones: Países por producto. (www.fao.org/faostat, fecha de consulta: 2017/11/14).

[27] Quintero-García S. L. & González-Salcedo L.O. (2006). Uso de fibra de estopa de coco para mejorar las propiedades mecánicas del concreto. Ingeniería y Desarrollo, 20:134-150

[28] Bastidas M., Buelvas L.M., Márquez M.I. & Rodríguez K. (2010). Producción de Carbón Activado a partir de Precursores Carbonosos del Departamento del Cesar, Colombia. Información Tecnológica, 21(3) ,87-96.

[29] SEMARNAT (Secretaria del Medio Ambiente y Recursos Naturales). (1996). NORMA Oficial Mexicana NOM-001-ECOL-1996 que establece los límites máximos permisibles de contaminantes en las descargas de aguas residuales en aguas y bienes nacionales. Diario Oficial de la Federación, segunda sección, México, 1-30.

[30] NMXAA-003. (1980). Mexican standard "residual waters.- sampling

[31] NMXAA-007 (2013).Water analysis - determination of temperatura In natural, residual and waste waters Treated - test method.

[32] NMXAA-008 (2016) Water analysis.- ph measurement in waters Natural, residual and waste treated. Test method- (cancel to the NMX-AA-008-SCFI-2011).

[33] NMX-AA-030/1-SCFI-2012 (2012). Water analysis-measurement of the chemical demand of oxygen in natural, wastewater and waste waste treated.- method of test-part 1-method of open reflux- (cancel to NMX-AA-030-SCFI-2001).

[34] Sing K.S.W., Everett D.H., Haul R.A.W., Moscou L., Pierotti R.A., Rouquerol J. & Siemieniewska T. (1985). Reporting physisorption data for gas/solid systems with special reference to the determination of surface area and porosity (recommendations 1984), Pure & Appl. Chem., 57(4), 603-619.

[35] Rout T., Pradhan D., Singh R.K. & Kumari N. (2015). Exhaustive study of products obtained from coconut shell pyrolysis. *Journal of Environmental Chemical Engineering*, 4(3), 3696-3705.

[36] Ouyang S., Xu S., Song N. & Jiao S. (2013). Coconut shell-based carbon adsorbents for ventilation air methane enrichment. *Fuel*, 113, 420-425.

[37] Ensuncho A.E., Milanés N. & Robles J.R. (2015). Remoción del Colorante Rojo Allura en Solución Acuosa utilizando Carbones Activados obtenidos de Desechos Agrícolas. *Información Tecnológica*, 26(2):69-78.

[38] Nahil M.A. & Williams P.T. (2011). Pore characteristics of activated carbons from the phosphoric acid chemical activation of cotton stalks. *Biomass and Bioenergy*, 37,142-149.

[39] Primera-Pedrozo O., Colpas-Castillo F., Meza-Fuentes E. & Fernández-Maestre R. (2011). Carbones activados a partir de bagazo de caña de azúcar y zuro de maíz para la adsorción de cadmio y plomo. *Revista de la Academia Colombiana de Ciencias Exactas, Físicas y Naturales*, 35(136):387-396.

[40] Daouda K., Ngomo-Manga H., Baçaoui A., Yaacoubi A. & Ketcha-Mbadcam J. (2013). Optimization of activated carbons prepared by and steam activation of oil palm shells. *Journal of Chemistry*. 2013(ID 654343), 1-10.

[41] Bhati S., Mahur J.S., Dixit S. & Chobey O.N. (2014). Study on effect of chemical impregnation on the surface and porous characteristics of activated carbon fabric prepared from viscose rayon. *Carbon Lett*, 15(1), 45-49

[42] Peña H., Karen J., Giraldo L. & Moreno, J. C. (2012). Preparación de carbón activado a partir de cáscara de naranja por activación química. Caracterización física y química. *Revista Colombiana de Química*, 41(2), 311-323.

[43] Chowdhury Z.Z., Zain S.M., Khan R.A., Islam M.S. & Arami-Niya A. (2011). Application of central composite design for preparation of Kenaf fiber based activated carbon for adsorption of manganese (II) ion. *International Journal of the Physical Sciences*, 6(31), 7191–7202.

[44] Sun Y., Yue Q., Gao B., Huang L., Xu X. & Li Q.(2012). Comparative study on characterization and adsorption properties of activated carbons with H_3PO_4 and $H_4P_2O_7$ activation employing Cyperus Alternifolius as a precursor. *Chemical Engineering Journal*, 181–182, 790–797.

[45] Sulistyani E., Tamado D.B., Wulandari F. & Budi, E. 2015. Coconut Shell Activated Carbon as an Alternative Renewable Energy. *KnE Energy*, 2, 6-81.

[46] Li L., Liu S. & Liu, J. (2011). Surface modification of coconut shell based activated carbon for the improvement of hydrophobic VOC removal. *Journal of Hazardous Materials*, 192, 683-690.

[47] Vacca V., Colina G., Rincón N., Díaz A., Behling E., Marín J., Chacín E. & Fernández N. (2012). Adsorption for the removal of phenolic compounds from the effluent of a biologic reactor. *Revista Técnica de Ingeniería Universidad del Zulia,* 35(3), 252-260.

[48] Rodríguez R.F. & Molina S. (1998). Carbones activados a partir de materiales lignocelulósicos . *Quibal. Química e Industria*, 45(9), 563-571.

[49] Huidobro, A., A. C., Pastor, F. & Rodríguez R. (2000). Preparation of Activated Carbon Cloth from Viscous Rayon. Part IV.*Chemical Activation Carbon,* 39 (3), 389-398.

[50] Rodríguez E.P., Giraldo L., & Moreno, J. C. (2011). Oxidación de la superficie de carbón activado mediante HNO3 y H2O2: efecto sobre la remoción de níquel (II) en solución acuosa. *Revista colombiana de química*, *40*(3), Pp. 349-364.

[51] Castells X. E. (2009). Reciclaje de residuos industriales. *Tecnologías aplicables para el tratamiento de residuos, su valorización y la fabricación de materiales a partir de residuos* (2da. Edición). Pp.60-67. Madrid. Editorial, Díaz Santos S. ISBN: 84-7978-437

[52] Rojas-Morales J.L., Gutiérrez-González E.C. & Colina-Andrade G.J. (2016). Obtención y caracterización de carbón activado obtenido de lodos de plantas de tratamiento de agua residual de una industria avícola. *Ingeniería Investigación y Tecnología*, 42(4) 453-462.